CSCE Annual Conference
Growing with youth – Croître avec les jeunes

Laval (Greater Montreal)
June 12 - 15, 2019

FLEXURAL BEHAVOIUR OF FIBER REINFORCED LIGHTWEIGHT SELF-CONSOLIDATING CONCRETE BEAMS

A. Ehsani Yeganeh[1, 2], A. Rashidian[1, 3], K. M. A. Hossain[1, 4],
[1] Department of Civil Engineering, Ryerson University, Canada
[2] ali.ehsaniyeganeh@ryerson.ca, [3] ali.rashidian@ryerson.ca, [4] ahossain@ryerson.ca

Abstract: This paper describes flexural behavior of fiber reinforced lightweight self-consolidating concrete (FRLWSCC) beams made of slag aggregates in combination with three different types of fibers such as: High-Density Poly Ethylene (HDPE), Crumb Rubber (CR) and Polyvinyl Alcohol (PVA). The performance of FRLWSCC beams compared to their lightweight self-consolidating concrete (LWSCC) counterparts are described based on load-deformation responses, stress-strain developments, crack characterization, failure modes, ductility and energy absorption capacity. All beams have shown flexural failure. Fiber reinforced beams have shown higher ultimate flexural capacity, higher deflection, ductility and higher energy absorption capacity with development of higher number of cracks and smaller crack widths compared to their LWSCC counterparts.

1 INTRODUCTION

Concrete can be mentioned as one of the most commonly used construction materials around the world (Sideris and Savva 2005, Ehsani Yeganeh 2015). Lightweight self-consolidating (LWSCC) and fiber reinforced lightweight self-consolidating concrete (FRLWSCC) are two of the latest innovations in self-consolidating concrete (SCC) productions which have combination of flowability of SCC, low dead weight of lightweight concrete (LWC) and ductility and mechanical improvement of fiber reinforced concrete (FRC) (Khayat and Roussel 2000, Ding et al. 2008, Aydin 2007, Nehdi and Ladanchuk 2004, Hassan et al. 2010).

LWSCC is capable of maximizing the structural efficiency by saving a large portion of total dead load of structures and foundations due to reduction of gravity load and seismic inertia mass (Corinaldesi and Moriconi, 2015, Hossain and Lachemi, 2007a). Furthermore, compared to traditional concrete, LWSCC has better quality of aggregate-paste contact zone (ITZ) due to its higher internal curing which leads to improve hardened properties and reduced concrete cracking (Lotfy et al. 2015, Hossain et al. 2011). Introduction of fiber into LWSCC is one of the most effective methods to improve the performance of concrete (under direct tensile and bending load) in terms of deformation/deflection before failure, crack propagation resistance, energy absorption, shrinkage and increased strain capacity provided by fiber reinforcement (Gonen 2015a, Hubertova and Hela 2007, Corinaldesi and Moriconi 2015, Lotfy et al. 2015, Sobhan and Mashnad 2002, Hossain and Lachemi, 2007b).

This paper presents the result of experimental study on the performance of FRLWSCC beams made of three different fibers such as: High-Density Poly Ethylene (HDPE), Crumb Rubber (CR) and Polyvinyl Alcohol (PVA) compare to LWSCC. As part of the experimental program, three FRLWSCC flexural beams and one LWSCC flexure beam with same dimensions were constructed.

2 EXPERIMENTAL PROGRAM

2.1 Description of test specimens

The experimental program has been devoted to investigating the structural performance of FRLWSCC flexural beams made of slag aggregates incorporating three different types of fibers such as HDPE, CR, PVA compared to those made with LWSCC with no fiber (tested as control specimens). In total four beams were designed based on CSA A23.3-04 (2004), casted and tested. As part of this experimental study, four singly reinforced beams were tested while the dimensions of the beams were kept constant at width, depth and length of 150 mm x 230 mm x 3300 mm, respectively as shown in Figure 1 and Figure 2. The longitudinal reinforcement consisted of 3-10M steel bars at bottom and 2-6M round steel bars at the top to hold the stirrups and adequate shear reinforcement (6M steel bars) was provided at a spacing of 60 mm c/c based on CSA A23.3-04 (2004).

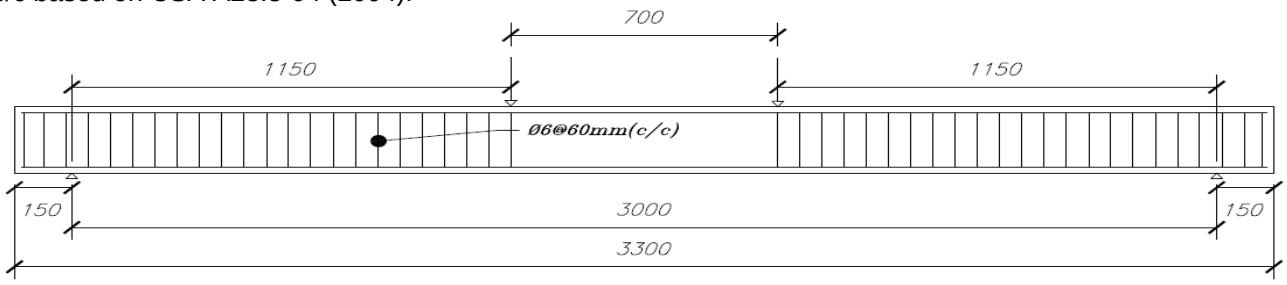

Figure 1: Schematic diagram of the geometry of Flexural beams

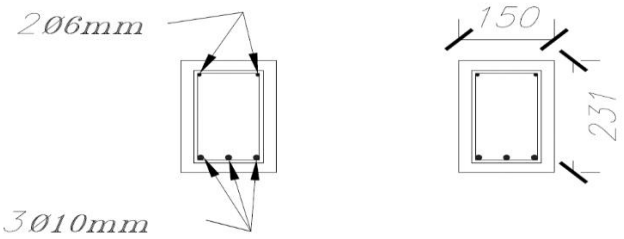

Figure 2: Cross-section of flexural beams

2.2 Material properties

For all FRLWSCC and LWSCC mixes, the water to cementitious material (w/b) ratio was 0.30. All mixes consisted of CSA type 10 or ASTM type 1 Portland cement, fly ash (class C), dry-densified silica fume (SF), water, coarse and fine slag aggregates with nominal size of 10 mm and 4.75 mm, respectively and poly carboxylate-based high range water reducer (HRWR). Due to high porous nature of lightweight aggregates, both coarse and fine aggregates had been pre-soaked in water for minimum of 72 hours and then 24 hours out of water in room temperature to let the excess water drained out and used the aggregates in saturated surface dry (SSD) condition. Loosing of fine particles during the procedure was avoided. Mix designs are provided in Table 1 while all three fibers are shown in Figure 3 and the geometrical and mechanical properties are presented in Table 2, respectively. A 350-liter shear mixer was used for mixing all concrete mixes. The slag coarse and fine aggregates were weighted in saturated surface dry (SSD) condition and introduced first into the mixer and mixed with 75% of water for 2 minutes at normal speed, then the rest of cementitious materials including fly ash, silica fume and cement were added and mixed for another 5 minutes. HRWRA slowly added to the mix with remained 25% water and mixed for another 5 minutes. Finally, fiber was added to the mixer and mixed for 15 minutes. Same procedure had been applied for LWSCC mix as well without mixing period for fibers.

Table 1 Concrete mix designs

Concrete Mix	w/b	cement	Fly Ash (Class C)	Silica fume	Water	Coarse Aggregate (SSD)	Fine Aggregate (SSD)	HRWR kg/m^3	Fiber kg/m^3
All Ingredients are calculated based on 1 part of cement									
1% HDPE-FRLWSCC	0.30	1.00	0.16	0.09	0.38	0.99	1.61	4.75	9.2
1% CR-FRLWSCC	0.30	1.00	0.16	0.09	0.38	0.99	1.61	4.75	9.2
0.5% PVA-LWSCC	0.30	1.00	0.16	0.09	0.38	0.99	1.62	4.75	6.5
LWSCC	0.30	1.00	0.15	0.09	0.37	1	1.61	4.75	0

Table 2: Geometrical and mechanical properties of fibers

Fiber type	Length (mm)	Specific Gravity ($\frac{Kg}{m^3}$)	Melting point (℃)	Diameter (Microns)
PVA	8	1.3	225	38
HDPE	0.1	0.96	135	5
Crumb rubber	0.4	0.9	N/A	2

Figure 3: HDPE, PVA and Crumb rubber fibers

The compressive strength of all concrete mixes were obtained from testing of control cylinders according to ASTM C39 (2003) and flexural strength were determined based on ASTM C78 (2010) at 28 days under four-point bending test. The four-point bending test was performed using a closed-loop controlled servo-hydraulic system under displacement condition at a loading rate of 0.005 mm/s. The total span length of the flexural specimens was 304.8 mm. Table 3 summarizes the concrete compressive strength, flexural strength and air dry density of tested samples. Load-deflection responses of all types of concretes based on flexural strength test are shown in Figure 4 (a-d).

Table 3: Concrete compressive strength, flexural strength and density at 28 days

Concrete	Mean compressive strength (MPa)	Mean flexural strength (MPa)	Mean air dry density (kg/m^3)
HDPE-LWSSC	38.7	2.8	1862
CR-LWSCC	46.7	2.8	1890
PVA-LWSCC	43.6	2.9	1810
LWSCC	52.6	2.3	1826

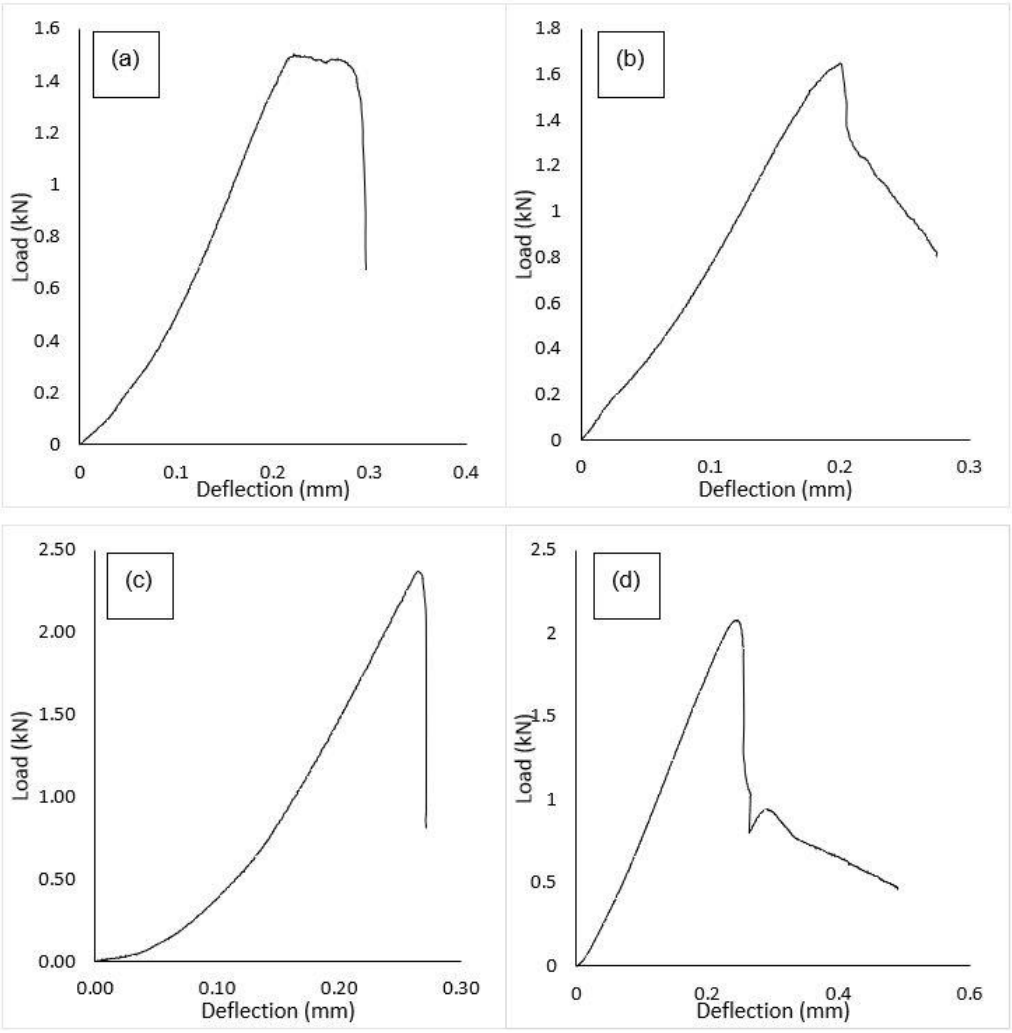

Figure 4: Load-deflection responses (a) LWSCC (b) CR-LWSCC (c) HDPE-LWSCC (d) PVA-LWSCC

Sample of stress-strain curves for steel reinforcement are shown in Figure 5 with yield stress and strain values are summarized in Table 4.

Table 4: Properties of steel reinforcement

Rebar	Yield strain (micro-strain)	Yield stress (MPa)
10 mm	2015	504
6 mm	---*	447

*: mechanical machine limitation

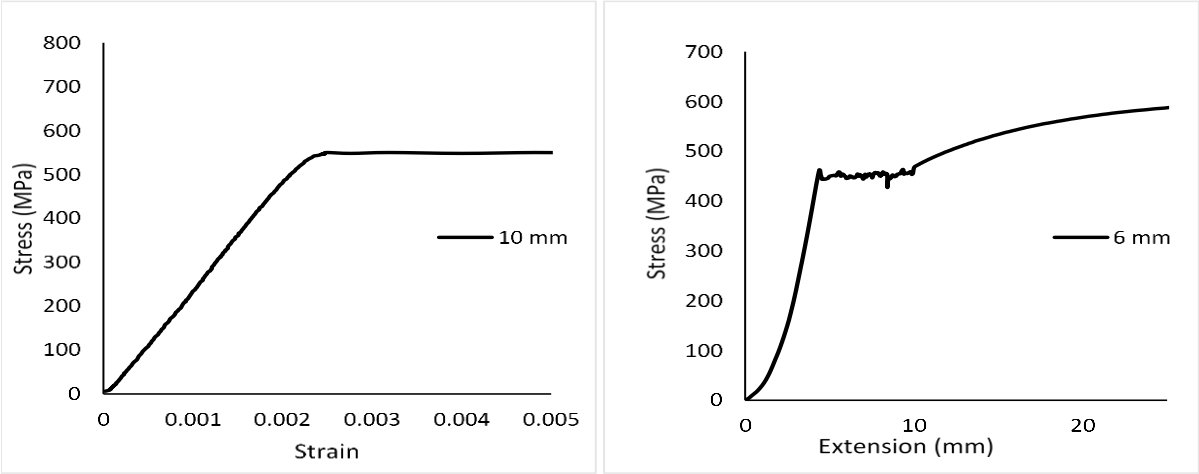

Figure 5: Rebar stress-strain/deformation responses of steel rebars

3 Results and discussion

3.1 Experimental results

Three singly reinforced FRLWSCC beams and one LWSCC beam as control were tested under four-point loading to failure. The reinforcement ratio and shear span to effective depth ratio (a/d) were kept constant at 1% and 5.75, respectively for all beams. Figure 6 (a-d) compare experimental load-deflection curves of all tested FRLWSCC and LWSCC beams. For all tested beams except CR-LWSCC beam, the maximum deflection values at mid-span (x = 1500 mm) were in the range of 42% to 66% higher than those recorded close to the support (x =750 mm and x=2250 mm, respectively) at failure stage. In case of CR-LWSCC beam, the maximum mid-span deflection was 31.4 mm which was 88% more than the obtained deflection value near each support which was 16.9 mm and 16.8 mm at x=750 mm and x = 2250 respectively at failure stage. Details of deflections at each location for all beams are provided in Table 5. The ultimate/peak moment capacity at failure stage of tested beams HDPE-LWSCC, CR-LWSCC, PVA-LWSCC and control LWSCC were 24.3 kNm, 24.9 kNm, 26.2 kNm and 24.2 kNm, respectively. The highest ultimate moment capacity of 26.2 kNm was obtained by PVA-LWSCC beam and the lowest ultimate moment value of 24.2 kNm was obtained by the LWSCC beam with corresponding mid-span deflections of 33.5 mm and 17.7 mm, respectively.

Table 5: Summary of loads, moment and failure modes of flexural beams

Beam code	Concrete compressive strength (MPa)	Failure mode	First flexural crack load* (kN)	Ultimate load (kN)	Ultimate Moment (kNm)	Deflection at ultimate load Du (mm)	Deflection at first flexural crack (mm)
HDPE-LWSCC	38.7	Flexural	5	42.2	24.3	29.3	1.6
CR-LWSCC	46.7	Flexural	10	43.3	24.9	31.3	4
PVA-LWSCC	43.6	Flexural	15	45.5	26.2	34.1	6
LWSCC	52.6	Flexural	8	42.0	24.2	17.7	1.5

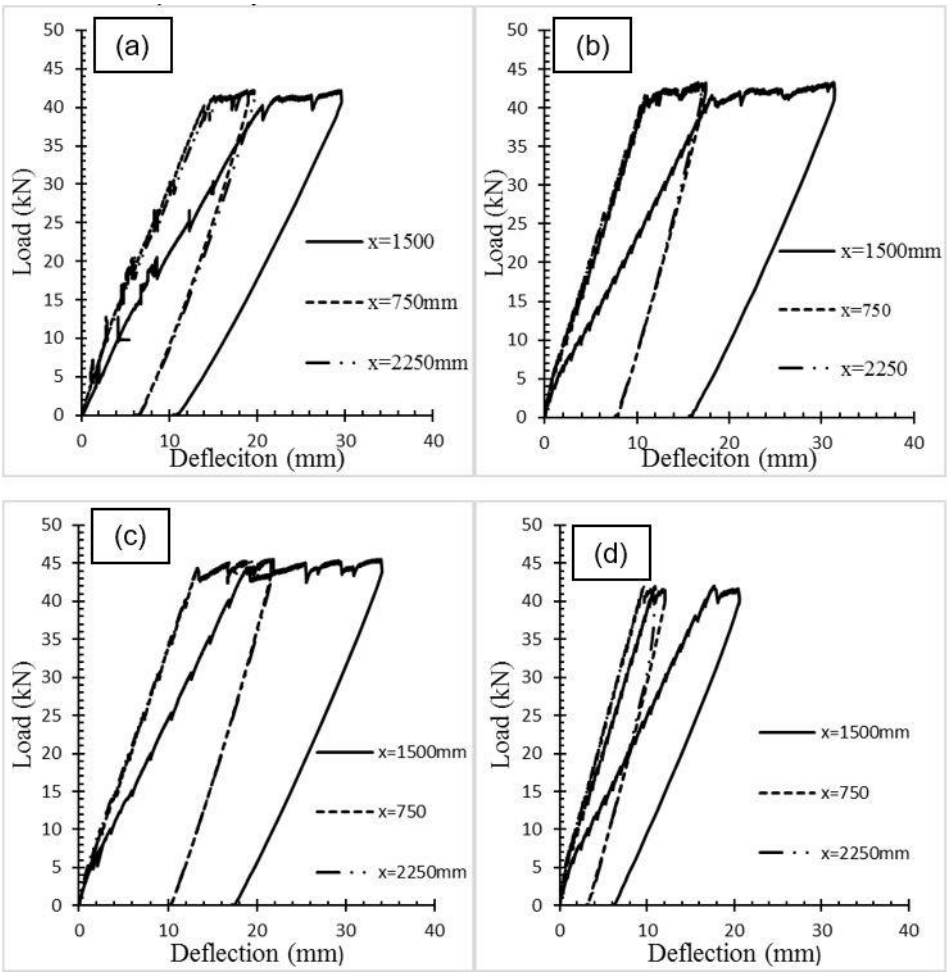

Figure 6: Load-deflection curves for tested flexural beams: (a) HDPE-LWSCC, (b) CR-LWSCC, (c) PVA-LWSCC and (d) LWSCC

3.2 Failure modes, crack pattern, crack width and number of cracks

The first flexural cracks were formed within the zero-shear region at mid-span of all beams at about 11.8% to 32% of the applied ultimate load. PVA-LWSCC had the highest first flexural crack load of 15 kN which was approximately twice that of the control beam with mid-span deflection of 6 mm which was considerably higher than the 1.5 mm deflection of the control beam. HDPE-LWSCC beam had lower first flexural crack load of 5 kN which was 40% lower than control LWSCC beam. With increasing applied load, new vertical flexural cracks were formed along the beam and the shear span. Due to higher deflection of PVA-LWSCC, formation of crack was distributed along the beam even close to the supports whereas for the LWSCC beams, most of the cracks were formed within the mid-span and propagated from the bottom (tension surface) of the beam towards the top (compression surface) with no flexural cracks identified close to the supports compared to all other FRLWSCC flexural beams. Details of crack pattern are shown in Figure 7(a-d).

Crack width, number of cracks, maximum crack width and type of failure cracks for all tested beam are provided in Table 6. PVA-LWSCC beam had the greatest number of cracks (46 cracks) with average crack width of 0.07 mm compared to other tested beams. HDPE-LWSCC beam had the smallest maximum crack width of 0.5 mm compared to those of other beam counterparts. Approximately all the tested beams had the same average crack width with only flexural crack type.

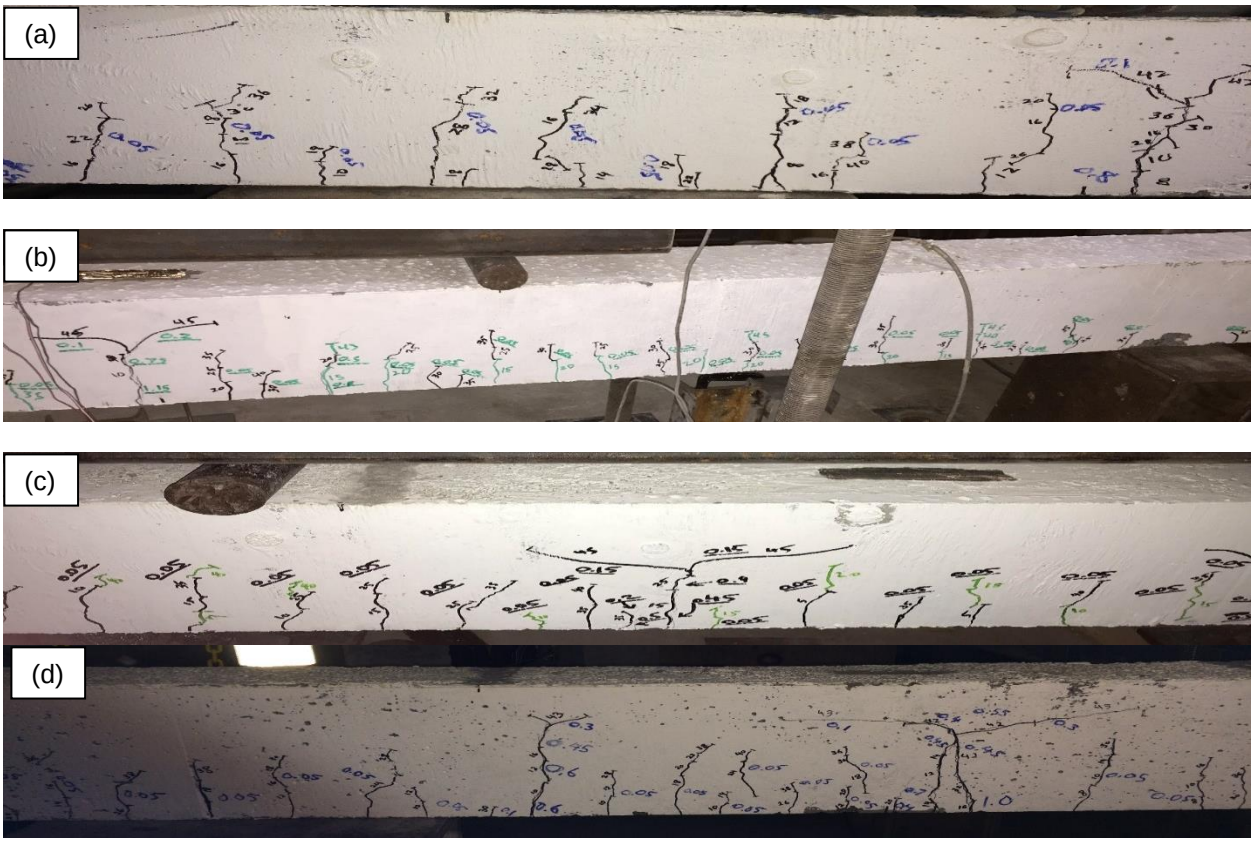

Figure 7: Crack patterns at the centre of flexural beams (a) CR-LWSCC, (b) LWSCC, (c) PVA-LWSCC and (d) HDPE-LWSCC

Table 6: Summery of crack width and number of flexural beams

Beam code	Number of cracks	Average crack width (mm)	Maximum crack width (mm)	Failure crack type
HDPE-LWSCC	42	0.05	0.5	Flexural crack
CR-LWSCC	39	0.05	1	Flexural crack
PVA-LWSCC	46	0.07	1	Flexural crack
LWSCC	36	0.05	0.8	Flexural crack

3.3 Strain development in concrete and flexural reinforcements

Figure 8 (a-d) shown the strain development of concrete at compression zone, during the loading history for FRLWSCC and LWSCC beams. The tensile strain developed gradually in bottom reinforcement with increase in the applied load and ended by yielding of the flexural reinforcement at ultimate stage. The load-strain response of CR-LWSCC and LWSCC beams showed that the obtained value of the developed strain in the top reinforcement and the concrete at compression were close as presented in Figure 8 (b) and 8 (d) which could be due to their similar distance from the natural axis.

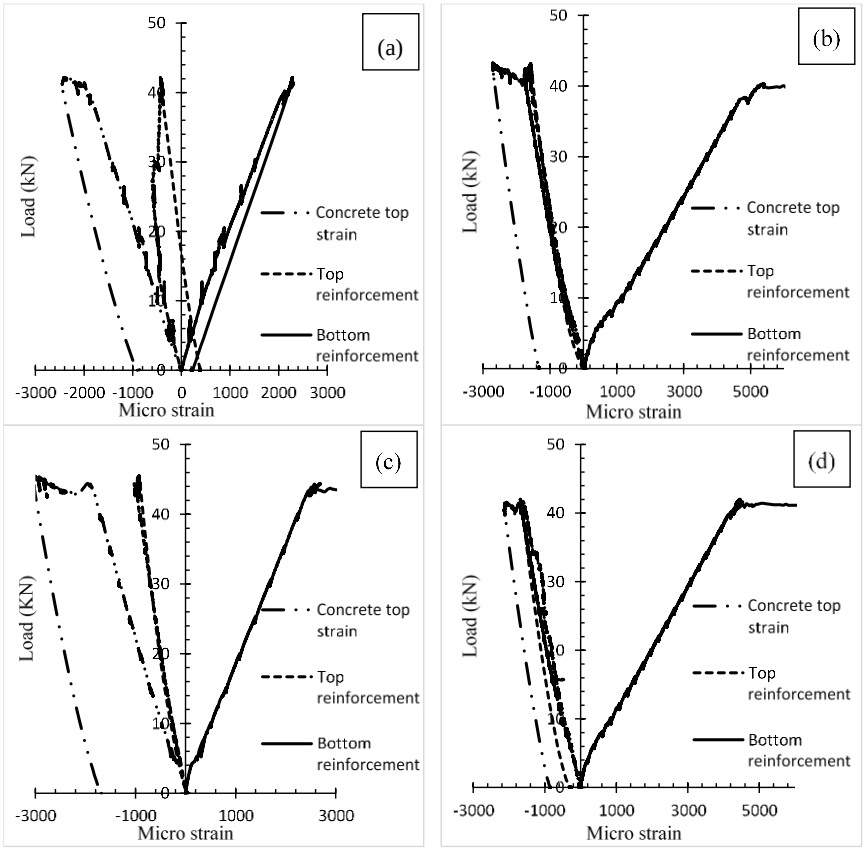

Figure 8: Load-strain curves for tested: (a) HDPE-LWSCC, (b) CR-LWSCC, (c) PVA-LWSCC and (d) LWSCC

Table 7 summarizes load at first steel yield, strain at yielding and ultimate stages and the ultimate failure load values for the tested FRLWSCC and LWSCC beams.

After the bottom reinforcement of HDPE-LWSCC and CR-LWSCC beams yielded, beams failed by increase of applied load, therefore the values of the load at first steel yielding were 6% and 14% lower than the ultimate load capacity, while the value of the concrete strain at compression zone were 2475 micro strain and 2667 micro strain, respectively.

Table 7: Summary of yield load, ultimate load/moment and strain for tested flexural beams

Beam	Load at first steel yielding (kN)	Yielding stage (beginning of large strain development) (micro strain)			Ultimate/failure stage strain (micro strain)			Ultimate Load, (kN)
		Bottom rebars	Top rebars	Concrete strain at compression	Bottom rebars	Top rebars	Concrete strain at compression	
HDPE-LWSCC	39.7	2281	381	1984	2285	444	2475	42.2
CR-LWSCC	37.2	5537	1516	1723	22295	1758	2667	43.3
PVA-LWSCC	45.5	2592	894	1889	15758	977	3003	45.5
LWSCC	42.0	4587	1677	2002	27499	1648	2129	42.0

In case of PVA-LWSCC and LWSCC, immediately after yielding of the flexural reinforcement the beam failed where the concrete strain value at compression were 3003 micro strain and 2129 micro strain which were found as the maximum and minimum obtained concrete strain among the tested beams, correspondingly. As per CSA A23.3-04. (2004) standards, the maximum concrete compressive strain is equal to 3500 micro strain at ultimate stage which the obtained results were within the specified limit.

3.4 Ductility behavior, energy absorption capacity and stiffness of FRLWSCC-F beams

Ductility of a member is defined based on the ability of a member to deform without a significant loss of its strength. Stiffness calculated from slope of flexural load-deflection curve. Energy absorption obtained from the area under flexural load-deflection curve up to the post peak flexural of 85% of the ultimate load. The ductility index (DI) here is defined as the ratio of deflection at failure/ultimate stage (D_u) to that at first yielding of steel (D_y). The ability of a member to absorb energy calculated from the area under the load–deflection responses is shown in Figure 7. PVA-LWSCC and CR-LWSCC beams had the highest energy absorption capacity which was 113% and 100% higher than control LWSCC beam, respectively. The control beam LWSCC was stiffer (stiffness of 4.26 N/mm) than other FRLWSCC beams as expected (Table 8). Existence of fiber in the concrete decreased the stiffness of flexural beams. Table 8 provides the DI values for FRLWSCC flexural beams based on D_y and D_u obtained from load–deflection responses shown in Figure 6. Generally, the ductility index is strongly affected by the crushing strain of concrete. PVA-LWSCC, CR-LWSCC beams showed better ductility with DI approximately equal to 2.0 compared to HDPE-LWSCC and LWSCC beams.

Table 8: Summery of ductility factor, energy absorption and stiffness of flexural beams

Beam code	Concrete compressive strength (f'c)	Peak/failure load (kN)	Ductility factor (DI)	Energy absorption (J)	Stiffness (N/mm)
HDPE-LWSCC	38.7	42.2	1.5	794.9	2.12
CR-LWSCC	46.7	43.3	1.9	1025.3	3.14
PVA-LWSCC	43.6	45.5	2.0	1084.6	2.82
LWSCC	52.6	42.0	1	508.2	4.26

4 Conclusion

The following conclusions are drawn from experimental results:

- All FRLWSCC beams showed typical structural behavior in flexure. Since beams were designed for steel yielding, therefore all longitudinal reinforcement at tension zone yielded before crushing of the compression concrete in pure bending region.
- Introducing fiber in LWSCC reduced the compressive strength but increased the ultimate load capacity of beams. PVA-LWSCC showed higher load capacity before concrete first flexural crack compared to other beams.
- All FRLWSCC beams had higher number of cracks and smaller crack widths compared with their control LWSCC counterpart.
- Beams with fiber showed higher concrete strain at failure stage with lower concrete strain at yielding stage compared to control ones without fiber.
- All FRLWSCC beams had higher ultimate load capacity, better ductility, higher deflection at ultimate load and higher moment capacity compared with LWSCC control beam. All FRLWSCC beams showed higher ability to absorb energy - energy absorption capacity was increased by 100% and had approximately 100% lower stiffness compared to control LWSCC beam.

5 Acknowledgement

The authors acknowledge the financial support provided by NSERC Canada and the support of Lafarge Canada for providing the lightweight aggregates.

6 References

ASTM C39, 2003. Standard test method for static modulus of elasticity and Poisson's ratio of concrete in compression. *American Society for Testing and Materials*, West Conshohocken, Pennsylvania, USA.

ASTM C78 / C78M, 2010, Standard Test Method for Flexural Strength of Concrete (Using Simple Beam with Third-Point Loading). *American Society for Testing and Materials*, West Conshohocken, Pennsylvania, USA.

Aydin, A.C. 2007. Self compact ability of high-volume hybrid fiber reinforced concrete. *Construction and Building Materials journal,* **21**(6), 1149–1154

Ehsani Yeganeh, A. 2015. Structral behavoiur of reinforced high performance concrete frames subjected to monotonic lateral loading, MASc thesis, Ryerson university, Toronto, Canada.

CSA Standard A23.3-04. 2010. *Concrete Design Handbook*, 10th edition, Ontario, Canada: CSA.

Corinaldesi, V., and Moriconi, G. 2015. Use of synthetic fibers in self-compacting lightweight aggregate concretes. *Journal of Building Engineering*, **4**, 247–254.

Ding, Y., Liu, S., Zhang, Y. and Thomas, A. 2008. The investigation on the workability of fiber cocktail reinforced self-compacting high-performance concrete. *Construction and Building Materials*, **22**(7), 1462–1470.

Gonen, T. 2015. Mechanical and fresh properties of fiber reinforced self-compacting lightweight concrete. *Scientia Iranica*, **22**, 313–318.

Hassan, A.A.A., Hossain, K.M.A., and Lachemi, M. 2010. Structural assessment of corroded self-consolidating concrete beams. *Engineering Structures*, **32**(3), 874–885.

Hossain, K.M.A., Ahmed, S., and Lachemi, M. 2011. Lightweight concrete incorporating pumice based blended cement and aggregate: Mechanical and durability characteristics. *Construction and Building Materials*, **25**(3), 1186–1195.

Hossain, K.M.A., and Lachemi, M. 2007a. Characteristics of Self-Consolidating Concrete Characteristics of Self-Consolidating Concrete Incorporating Volcanic Ash. CI-Premier PTE LTD, 32nd Conference.

Hossain, K.M.A., and Lachemi, M. 2007b. Mixture design, strength, durability, and fire resistance of lightweight pumice concrete. *ACI Materials Journal*, **104**(5), 449–457.

Hubertova, M., and Hela, R., 2007. The Effect of Metakaolin and Silica Fume on the Properties of Lightweight Self-Consolidating Concrete. *ACI Materials Journal*, 35-48.

Khayat, K.H., and Roussel, Y. 2000. Testing and performance of fiber-reinforced self-consolidating concrete. *Materials and structures*, **33**(6): 391–397.

Lotfy, A., Hossain, K.M.A., and Lachemi, M. 2015. Lightweight Self-consolidating Concrete with Expanded Shale Aggregates: Modelling and Optimization. *International Journal of Concrete Structures and Materials*, **9**(2), 185–206.

Nehdi, M., and Ladanchuk, J.D. 2004. Fiber synergy in fiber-reinforced self-consolidating concrete. *ACI materials journal*, **101**(6), 508–517.

Sideris, K.K., and Savva, A.E. 2005. Durability of mixtures containing calcium nitrite based corrosion inhibitor. *Cement and Concrete Composites*, **27**(2): 277–287.

Sobhan, K., and Mashnad, M. 2002. Tensile Strength and Toughness of Soil–Cement–Fly-Ash Composite Reinforced with Recycled High-Density Polyethylene Strips. *Journal of Materials in Civil Engineering*, **14**(2), 177–184.